Optimization of an Oil and Gas Separation Plant for Different Reservoir Fluids Using an Evolutionary Algorithm

Olsen, Erik R.; Hooghoudt, Jan Otto; Maschietti, Marco; Andreasen, Anders

Published in:
Energy and Fuels

DOI (link to publication from Publisher):
10.1021/acs.energyfuels.0c04284

Publication date:
2021

Document Version
Accepted author manuscript, peer reviewed version

Optimization of an Oil and Gas Separation Plant for Different Reservoir Fluids using an Evolutionary Algorithm

Erik R. Olsen,[†] Jan-Otto Hooghoudt,[‡,§] Marco Maschietti,[†] and Anders Andreasen[*,¶]

[†]*Aalborg University, Department of Chemistry and Bioscience, Niels Bohrs Vej 8, DK-6700 Esbjerg, Denmark*

[‡]*Aalborg University, Department of Mathematical Sciences, Skjernvej 4A, DK-9220 Aalborg Ø, Denmark*

[¶]*Ramboll Energy, Field Development, Studies and FEED, Bavnehøjvej 5, DK-6700 Esbjerg, Denmark*

[§]*Current address: Novo Nordisk, Alfred Nobels Vej 27, DK-9220 Aalborg Ø, Denmark*

E-mail: anra@ramboll.com

Abstract

The optimization of an oil and gas separation plant operating revenue has been performed for different characteristic reservoir fluid types (gas condensate, volatile oil and black oil) using an evolutionary algorithm. A process simulation model mimicking a typical plant has been used as a black-box model and optimized with respect to nine design variables using the CMA-ES algorithm. The plant studied has three separation stages, including gas re-compression for each stage as well as a final gas boosting step before export. Each compression stage includes gas cooling and partial condensation

upstream compressors. All condensate streams from the re-compression system are recycled back into the separation system for increased liquid recovery. The results indicate the following common optimal settings among others: the first stage temperature is optimal at the high bound, the third stage temperature is optimal at the low bound, the temperature of the gas from the middle stage separator is optimal at the lower bound. Some of the settings are different between the three fluids investigated, but with a clear trend among the fluids. One example is the optimal middle stage separator pressure, which increases with decreasing gas-oil ratio of the fluid. Benchmarking the optimization potential indicates that an increased operating revenue of close to 1% may be realized for the gas condensate and the volatile oil, whereas the optimization potential is less for a black oil fluid type. It is also noted that this optimization may come at a significant penalty in terms of the energy required, especially for the volatile oil case.

Introduction

The separation of reservoir fluids from production wells into separate gas and liquid phases is performed in surface facilities, both offshore as well as onshore, consisting of a number of separation stages where oil and gas (and usually also produced water) are separated. The fluids usually pass through 2-4 separators, where the liquid from one separator is passed to the next. For each stage, the pressure is reduced to gradually liberate more and more gas until a sufficiently stabilized liquid product is formed suitable for export via pipeline, for temporary storage, or for further processing in downstream refinery. The quality of the stabilized liquid product is often set to meet specific requirements in terms of the amount of lighter fractions of hydrocarbons that may flash off. This is typically defined by a TVP (True Vapor Pressure) and/or an RVP (Reid Vapor Pressure) target, and this is one of the most important constraints for such a facility. The gas liberated from each separation stage is re-compressed and the total amount of associated gas can be used for a number of

different purposes such as fuel gas for local power generation, gas lift, gas reinjection, gas export or, as a last resort, flaring. For gas export via pipeline, the specification made by the gas shipper or receiving facilities often induces requirements for dehydration, gas sweetening and hydrocarbon dew point control of the gas.[1]

The optimization of surface facilities for the separation of reservoir fluids into separate liquid and gaseous phases has been of scientific and practical interest for decades. The objective is traditionally to maximize the liquid volume for a given fluid flow into the surface facilities. The liquid export stream is more valuable, especially when no gas export route exists and excess gas is flared, but often also even with gas exported to sales. Earlier studies focused on finding optimal pressure in the separators constituting the separation train (consecutive gas/liquid separators), but estimation of the optimal number of separators has also been of interest. More separation stages will increase the liquid recoverable amount, but as more and more stages are added, the incremental change decreases.[2,3] Often an optimum is found between 2-4 stages considering CAPEX and OPEX, and for offshore facilities, also lay out considerations.

In terms of optimal separator pressures, the target of several studies has been to provide engineering calculations, which could guide the designers and operators in selecting the best settings. Traditionally, many surface facilities have not included a compression system due to the lack of a gas export route. Inclusion of a gas compression system is more and more common, either due to the need for high pressure gas lift or if a gas export route has been established, or both. The associated gas, even for crude oil / volatile oil, is considered valuable. Furthermore, it is not considered environmentally acceptable to flare gas.

The existence of a compression system on top of the separation train greatly increases the complexity of the plant and increases the number of adjustable variables greatly. In the compression system more liquid condensate streams may also exist due to cooling and subsequent partial condensation. These streams are often recycled back into lower pressure gas/liquid separators to increase the overall liquid recovery and to avoid disposal of valuable

product. These condensate streams often carry C_1-C_5 components and are often heavy in NGL (natural gas liquids, C_2-C_4). These components also constitute the majority of the gas phase flashed in the downstream gas/liquid separators. For such a facility, there will often be a significant recycling of lighter components, which flash from the reservoir fluid, then enter the compression system, where condensation by cooling occurs, and then some of these components are fed back into the separation train. Thus, in such complex facilities, it is easy to imagine that optimizing the separator pressure(s) alone may lead to sub-optimal settings, if settings of the individual parts of the compression system are not included. This is mostly due to, but not limited to, the temperature of the gas streams entering individual compressors. Thus, to find optimal settings, a plant-wide approach (in this context considering both the separation train and the compression train) is required.

Comprehensive reviews of the literature regarding optimization of surface facilities have recently been given by Mahmoud *et al.*[4] and Andreasen,[5] and here we elaborate by providing an overview of the different approaches, which have been taken in order to perform optimization of surface facilities, cf. Table 1.

The references in Table 1 span a wide range in terms of optimization methods and modeling complexity. For the optimization methods applied, the full range from brute force and one factor at a time (OFAT), deterministic gradient based approaches, to stochastic evolutionary algorithms as well as artificial neural networks (ANN) is covered. The optimization problem may be defined as a local optimization, i.e. only a few variables in a few separation stages or with settings for one type of equipment only to a plant-wide optimization approach (PWO), where more or less the entire process plant and relevant settings for temperature and pressure are taken into consideration. The model itself, which is used as the basis for optimization may range from a user defined (UDF) flash routine based on equation of state (EOS) for a single point in a process to a full-fledged flow sheeting process simulation model, often using commercial specialized software. Some studies also base the optimization on reduced order models, i.e. surrogate models where a more complex behavior/simulation is

Table 1: Overview of representative works related to optimization of surface oil and gas separation system optimization.

Simulation Purpose	Optimization algorithm	Model	Number of separation stages	Compression system. included	Condensate recycle included	Gas conditioning included	Number of variables	Number of fluids	Year	Ref.
PWO	EA[1]	Full sim.	3	yes	yes	no	9	3	2020	This work
PWO	EA[2]	Full sim. +Kriging	3	yes	yes	yes	10	1	2020	[5]
Local	Brute Force	Full sim.	1-4	yes	no	no	1-4	2	2019	[2]
PWO	EA[3]	Full sim.	3	partial	no	[a]	3-4[b]	1(3)[c]	2019	[6]
Local	GA	Full sim.	3-5	yes	no	no	3-5	1	2019	[3]
PWO	SLSQP	RSM	3	yes	yes	yes	5	1	2018	[7]
PWO	EA	Full sim.	3	partial	no	[a]	7	1	2018	[8]
PWO	EA[a]	Full sim.	3/4	yes	no/yes	no	9	1	2014	[9]
Local	GA	Full sim.	3/4	no	no	no	3/4	2	2014	[10]
Local	OFAT	UDF EOS	2/3	no	no	no	1/2	2	2013	[11]
Local	Deterministic	UDF EOS	2–5	no	no	no	4–7		2010	[12]
Local	Brute Force	UDF EOS	3	no/yes	no	no	2/4	3	2009	[13]
Local	OFAT	UDF EOS	4	no	no	no	3	1	2008	[14]
Local	ANN	Correlation	3	no	no	no		Mult.	2006	[15]

Notes:
1. CMA-ES, 2. NSGA-II, 3. NSGA-II/SQP hybrid
a. The plant includes gas conditioning, but it is unclear if this part has been included in the modeling.
b. 8 variables included in screening, but reduced when running the optimization.
c. Three different production scenarios investigated with the same reservoir fluid.
Abbreviations:
PWO: Plant Wide Optimization, EA: Evolutionary Algorithm, GA: Genetic Algorithm, SQP: Sequential Quadratic Programming, SLSQP: Sequential Least-Squares Programming, OFAT: One Factor A Time, ANN: Artificial Neural Network, NSGA: Non-dominant Sorting Genetic Algorithm, CMA-ES: Covariance Matrix Adaption Evolution Strategy, RSM: Response Surface Methodology/modeling, UDF: User Defined Flash, EOS: Equation of State.

represented by: a correlation, a response surface (RSM), a Kriging model, ANN or other Machine Learning methods. Such representation has the benefit of providing either analytical derivatives or smooth numerical derivatives, which opens up for a wider range of optimization methods and/or significantly reduced simulation times. The number of separation stages varies from 1–5 with 3–4 being the most common. Some problems consider only the separation train, while some include the compression train. A subset of these also takes the gas conditioning/dew-pointing facility into account. Most studies consider only a single type of fluid, although a few studies consider 2 or 3 different fluid types. A single study considers a multitude of fluids with different properties. It seems common, that when more fluid types are considered, the modeling complexity is reduced in some way, e.g. the gas compression system is excluded, or the number of variables is reduced. The number of variables spans a range from a single variable (middle separator pressure) to 8-10 variables in recent studies that utilize a plant-wide approach.

Generally, the optimizations are constrained to some extent, either in variables/factors or responses. For instance, an intermediate separation stage will be constrained to a pressure, which is in-between the upstream and downstream separator pressures. Furthermore, the quality of the produced oil is subject to a maximum allowable bubble-point pressure, typically given by TVP, or indirectly RVP.

In the present study, we utilize a plant-wide approach for optimizing a typical offshore oil and gas separation plant for three different reservoir fluids, the archetypes: gas condensate, volatile oil and black oil. A simulation model including both a separation train as well as a compression train will be considered, which also takes into account internal recycle streams due to partial condensation in compressor suction scrubbers, which are recycled to the separation train. We utilize a stochastic method in the form of an evolutionary algorithm treating the plant simulation model as a black-box. This work is a natural extension of our previous works[2,5,7] bringing it to a higher combined complexity.

By combining a relatively high number of process variables using a plant-wide approach and by considering three different archetypes of reservoir fluids, this study aims at highlighting trends, differences and similarities in optimal operating parameters for the separation of the given fluid archetypes. Such information is deemed valuable both when designing facilities for a specific fluid type and when adjusting the operating parameters if the wellfluid changes over lifetime or if other wellfluid types are introduced due to e.g. tie-back of new producing wells/reservoirs.

Methods

Process description

A typical oil and gas separation plant is modeled with some simplifications such as the lack of gas dehydration and gas treatment (dew point control). The process consists of an oil and gas separation train coupled with gas re-compression. The separation train is a multistage

process, where the feed mixture is progressively depressurized and concurrently gas and liquid phases are separated. The process flow diagram (PFD) of the system under investigation is shown in Figure 1. Because the focus of this work is on the optimal separation of gas and oil, the feed is considered water-free, and all separators are modeled as 2-phase separators. Each stage consists of an isenthalpic (PH-flash) expansion followed by gas-oil separation. The oil exiting a separator is further depressurized and fed to the immediate downstream separator with the exception of the oil exiting the last separator of the train, which is exported or routed to tank. In this work, the separation train is composed of three stages. As shown in Figure 1, the separators are named S_1, S_2, and S_3. The possibility of regulating the temperature of these separators is provided for by heat exchangers upstream each separation stage. The saturated gas exiting each separator is cooled down, whereby condensation may take place. The condensates, if any, are separated from the gas in additional separators (compressor suction scrubbers) (S_{11}, S_{21}, S_{31}) and recycled back into the separation train. The condensates recovered in the separators S_{i1} are recycled back into the separation train at the stage $i+1$ except for the last stage, where the condensate is recycled into the same stage (see Figure 1) by means of pumping. The gas streams exiting the separators/scrubbers S_{21} and S_{31} are compressed up to the pressure of the preceding stage of the separation train, then cooled down and fed to the scrubbers/separators S_{11} and S_{21}, respectively. The gas exiting the scrubber/separator S_{11} is fed to a 2-stage re-compression where the pressure is increased up to the export pressure. This process setup is used for the optimization of all reservoir fluids.

Fluid description and simulation tool

Three optimization studies are considered in this work, corresponding to three distinct reservoir fluids: gas condensate, volatile oil and black oil. The composition of the fluids is taken from the literature[16] and presented in Table 2. The components up to C_5 are real single components (alkanes), i.e. methane, ethane, propane, i-butane, n-butane, i-pentane, n-pentane,

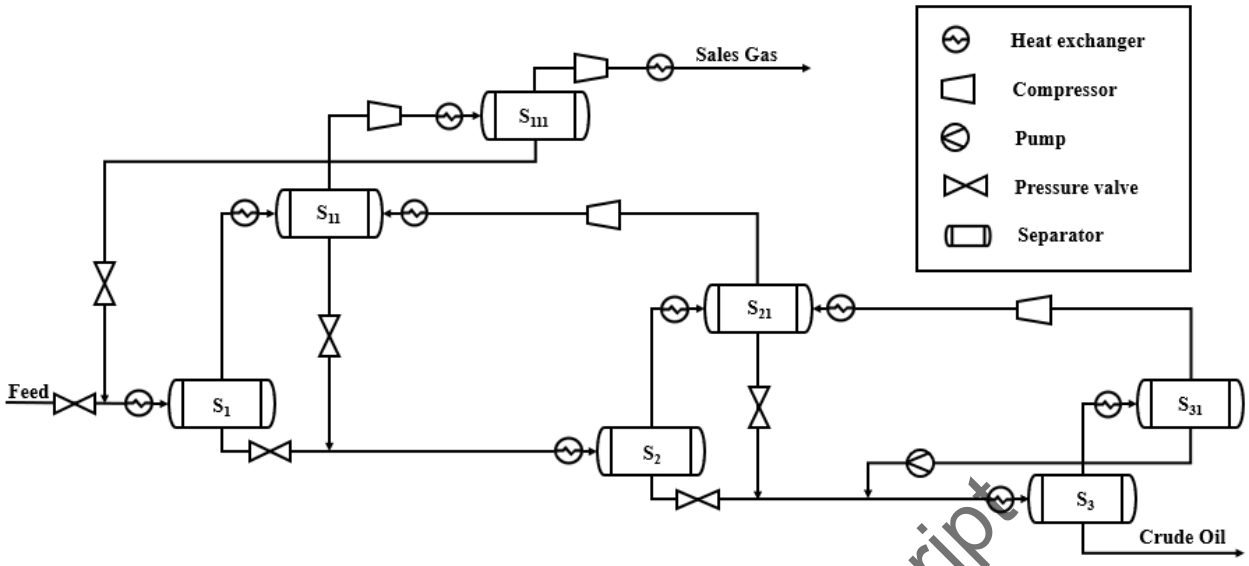

Figure 1: Process Flow Diagram of the system under investigation, consisting of a separation train coupled with a multi-stage gas re-compression train.

whereas the components from C_6 to C_{19} are pseudo-components representing hydrocarbon fractions of given carbon atoms. The components C_{20} and heavier are lumped as a single pseudo-component. Average molecular mass and specific gravity (SG) (at 60°F) for the pseudo-components C_7 and heavier are also reported in Bahadori[16] and reported in Table 2. Since average molecular mass and specific gravity for the C_6 fraction is not provided in ref.[16] the parameters for these fractions were assumed to be the same as those reported for one C_6 fraction reported by Danesh.[17] Table 2 also reports the GOR (gas-oil-ratio) and the liquid and gas density obtained via a flash calculation at standard conditions.

The process simulations are carried out using Honeywell Unisim Design R471 (Honeywell, Charlotte, North Carolina, US) using the Peng-Robinson equation of state[18] and COSTALD liquid density[19] for the thermodynamic calculations. The critical parameters (critical pressure, critical temperature, critical volume and acentric factors) for defined components were estimated internally by Unisim using the Twu method.[20,21] The corresponding phase envelopes for the three fluids investigated are depicted in Figure 2.

Table 2: Composition of the three archetype reservoir fluids, together with average molar mass and specific gravity (at 60°F) for pseudo-components C_6 and heavier. Additional characterization properties given for single stage stabilization at atmospheric pressure and 15.6°C.

		Gas condensate			Volatile oil			Black Oil		
Component group	Component name	Mole (%)	Molar mass (g/mol)	Specific gravity	Mole (%)	Molar mass (g/mol)	Specific gravity	Mole (%)	Molar mass (g/mol)	Specific gravity
Defined	N_2	0.60			0.58			0.56		
	CO_2	3.34			3.27			3.55		
	C_1	74.16			53.89			45.34		
	C_2	7.90			8.57			5.48		
	C_3	4.15			6.05			3.70		
	iC_4	0.71			1.05			0.70		
	nC_4	1.44			2.44			1.65		
	iC_5	0.53			0.88			0.73		
	nC_5	0.66			1.17			0.87		
Pseudo	C_6	0.81	84.0	0.69	1.45	84.0	0.69	1.33	84.0	0.69
	C_7	1.20	91.2	0.73	2.38	91.9	0.74	2.73	89.9	0.76
	C_8	1.15	104.0	0.77	2.59	104.7	0.765	3.26	103.2	0.78
	C_9	0.63	119.0	0.79	1.75	119.2	0.79	2.14	117.7	0.80
	C_{10}	0.5	133.0	0.80	1.50	131.0	0.79	1.94	133.0	0.80
	C_{11}	0.29	144.0	0.79	1.55	147.0	0.80	1.62	147.0	0.80
	C_{12}	0.27	155.0	0.80	0.93	161.0	0.81	1.47	160.0	0.82
	C_{13}	0.28	168.0	0.81	1.13	171.0	0.83	1.69	172.0	0.83
	C_{14}	0.22	181.0	0.82	1.01	182.0	0.84	1.62	186.0	0.84
	C_{15}	0.17	195.0	0.83	0.80	195.0	0.84	1.59	200.0	0.85
	C_{16}	0.15	204.0	0.84	0.86	208.0	0.85	1.30	213.0	0.86
	C_{17}	0.14	224.0	0.84	0.60	228.0	0.84	1.11	233.0	0.85
	C_{18}	0.09	234.0	0.84	0.68	247.0	0.85	1.26	247.0	0.86
	C_{19}	0.13	248.0	0.84	0.54	252.0	0.86	1.07	258.0	0.87
	C_{20+}	0.47	362.0	0.88	4.34	411.0	0.90	13.32	421.0	0.91
GOR	(Sm^3/Sm^3)			2313			358			134
SG(gas)	(–)			0.78			0.86			0.82
ρ(oil)	(kg/m^3)			830			846			866

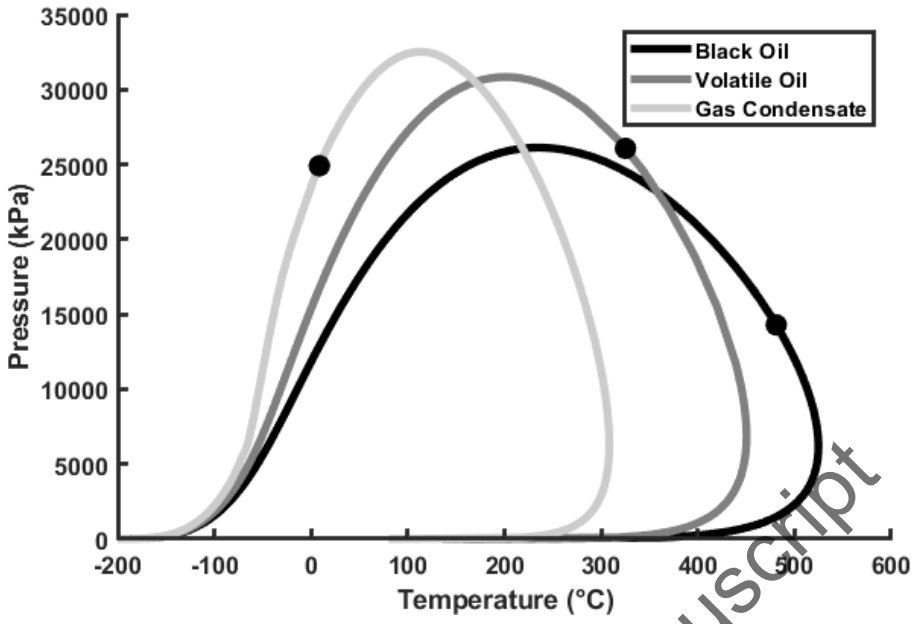

Figure 2: Calculated phase envelopes for the three fluids investigated. The critical point is marked with a filled circle for each fluid.

Definition of the optimization problem

The objective of the optimization is stated as the maximization of the net operating profit ϕ, defined as the revenues from oil ϕ_{oil} and gas ϕ_{gas} sales minus the operating expenses and expressed as \$ per unit mass of feed in kg. The sales price of the oil and gas was set to constant values, being 62.71 \$ per barrel oil and 2.61 \$ per MMBtu gas.[22] The revenues for the oil and gas per unit mass of feed were thus calculated by:

$$\phi_{\text{oil}} = \frac{F_{\text{oil}}}{F_f} \frac{394.4 \text{ \$/m}^3}{\rho_{\text{oil}}} \quad (1)$$

$$\phi_{\text{gas}} = \frac{F_{\text{gas}}}{F_f} \frac{0.092 \text{ \$/m}^3}{\rho_{\text{gas}}} \quad (2)$$

$$\phi = \phi_{\text{oil}} + \phi_{\text{gas}} \quad (3)$$

where F_f, F_{oil} and F_{gas} are the mass flow rates of the feed, the oil export and the export gas, respectively, in kg/hour, ρ_{oil} and ρ_{gas} are the densities of the export oil and the export

gas, respectively, in kg/m^3. The operating expenses included in the optimization are those related to the gas compression and to heating or cooling of the process fluids. All power requirements have been assumed to be internally covered by a fraction of the export gas: $P = F_{fuel} \cdot LHV \cdot \eta$, used as fuel gas, where P is the power requirement, F_{fuel} is the mass flow rate of the fuel gas required internal energy needs and η is an overall efficiency of the conversion of fuel to electrical power. The gas required for fuel gas is subtracted from the total gas production, and hence the export gas rate is given by:

$$F_{gas} = F_{gas,total} - F_{fuel} \tag{4}$$

Therefore, the energy expenditures (OPEX) results in a decrease in the gas revenues.

With regards to the gas compression, the adiabatic efficiency of all compressors was set to 0.75. As regards the coolers, seawater was used as cooling medium assuming that the seawater lift is the only term taken into account as energy requirement. Seawater temperature was fixed at 10 °C, with $\Delta T = 10$ °C of the seawater inside the coolers. The needed mass flow rate of seawater was then calculated by equating the heat duties process-side and seawater-side. For the duty calculations, the heat capacity of the process fluid was calculated by the property package of Honeywell Unisim Design, whereas the heat capacity of the cooling water was taken to be equal to 4.18 kJ/kg K. The density of the cooling water was assumed equal to 1000 kg/m^3. A pump head of 40 m was assumed for estimation of power requirement. The OPEX related to cooling is simply taken as the power requirements for pumpimg the cooling medium as well as the external seawater pumping. Likewise, the heating medium is assumed to be heated by waste heat from the power generation exhaust gas, and thus the OPEX related to heating medium is for simplicity also assumed to be limited to the circulation pump power requirement.

In the optimization, the variables shown in Table 3 are optimized in order to find the highest profit. Upstream the final compression stage (export compressor), the gas is cooled

down to 25 °C. The pressure in S_{111} i.e. on the suction side of the final compression stage is set as the geometric average between the export pressure, which is fixed at 120 bar, and the pressure in S_{11}. The main constraint in the present simulation study is the oil export specification, which states that the RVP of the export oil must not exceed 12 psia. The only other constraints are that the pressure in the separator stages must be lowered for each stage as the fluid moves forward in the separation train.

Table 3: Variables used in the optimization including upper and lower bounds.

Variable	Unit	Scaled variable	Lower	Upper	Description
P_S1	(kPa)	x(1)	1250	3500	1. stage separator pressure
P_S2	(kPa)	x(2)	300	3000	2. stage separator pressure
P_S3	(kPa)	x(3)	100	1000	3. stage separator pressure
T_S11	(°C)	x(4)	25.0	70.0	1. stage scrubber temperature
T_S21	(°C)	x(5)	25.0	70.0	2. stage scrubber temperature
T_S31	(°C)	x(6)	25.0	70.0	3. stage scrubber temperature
T_S1	(°C)	x(7)	33.0	60.0	1. stage separator temperature
T_S2	(°C)	x(8)	33.0	60.0	2. stage separator temperature
T_S3	(°C)	x(9)	33.0	60.0	3. stage separator temperature

Optimization strategy and setup

The strategy for optimization of the objective function utilizes the method of black-box optimization. Black-box optimization is often the preferred choice, and sometimes the only choice, when analytical derivatives are not available and when numerical estimation of derivatives is difficult. For process simulation solvers using a sequential solver the recycles/tear streams may likely cause noisy numerical derivatives.[23,24]

We apply the method of Covariance Matrix Adaptation Evolution strategy (CMA-ES) to find solutions for the various optimization problems. The CMA-ES method is a straightforward and very effective optimization strategy. The CMA-ES algorithm is very convenient since it has minimal parameters to be set by the user, can be run with default settings with good results, and does not require parameter tuning. In addition, the CMA-ES has been used for a similar application with success[9] and studies also indicate that CMA-ES has good

performance compared to other algorithms.[25,26] The strength of the method relies on a smart generation of phase-space points (seeds) applied to probe the phase space in an effective way in search of local/global maxima. Briefly, a population of phase space points (seeds) are iteratively generated by sampling from a multivariate normal distribution—with its corresponding mean and covariance matrix updated at each step in the iteration process—until the method converges to a local maximum or to the global maximum. That is at each step $k+1$, M state-vectors (seeds) $\mathbf{x}$ are generated by sampling from a multivariate normal distribution defined by the mean $\bar{x}^k$ and the covariance matrix Σ^k, that is $\mathbf{x}_i^{k+1} \sim \bar{\mathbf{x}}^k + N(0, \Sigma^k), k = 0, 1, 2, \ldots$ and $i = 1, \ldots, N$. The value of $\bar{x}^k$ is computed by a weighted average of a subset of the $\mathbf{x}_i^k$ as generated on step k, where the subset is taken to consist of $L < N$ state-vectors $\mathbf{x}_i^k$ displaying the highest value of the objective function at step k. Updating of the covariance matrix Σ^k is mathematically more involved and is thoroughly discussed in various works by Hansen and coworkers.[27–31] Standard software implementation is readily available, and the Matlab/Octave implementation by the *cmaes.m* function[32] has been used in this study.

The applied code re-samples by default when the objective function returns NaN, a convenient functionality in order to deal with some of the constraints we encounter in our optimization problem. Each variable is scaled to lie between [1:10]. For each investigated reservoir fluid the default population size is $\lambda = 4 + \lfloor 3 \log(N) \rfloor$, where N is the number of variables.

One of the constraints is that the pressure in each separator must be lower than in the previous separator. This constraint is conveniently implemented by generating NaN in the objective function code in such cases, and the CMA algorithm generates a new seed, thereby excluding such prohibited phase space points. The RVP constraint of 12 psia can only be evaluated after the computation performed by Unisim Design. In case of violation, this is handled by gradually penalizing the objective function depending on the distance from RVP of 12 psia. No penalty is applied for RVP $<$ 12 psia and then the objective function equals $f(\mathbf{x})$ while otherwise it equals $f(\mathbf{x})$ divided by 1+(RVP-12).

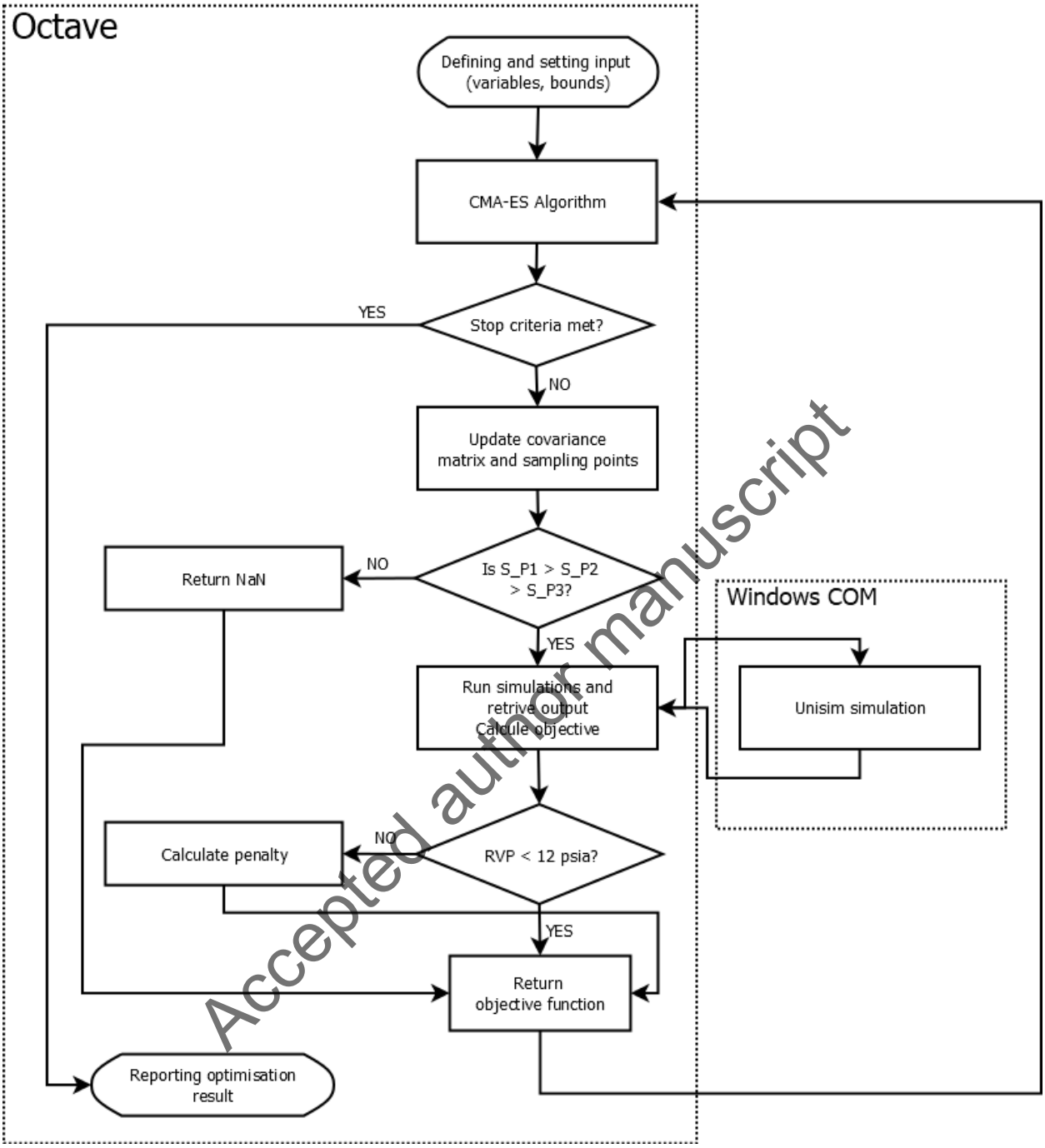

Figure 3: Schematic of computational setup.

An objective function is coded, wrapping calls to the process simulation in Matlab[33]/Octave.[34,35] The calls to and from the Honeywell Unisim Design simulation are performed using the Windows Component Object Model.[36] A similar coding and black-box approach for performing optimization using a commercial process simulator has been used by others, utilizing e.g.

VBA, Matlab and python.[5,9,23,24] The computational setup and flow of the optimization is visualized in Figure 3. The main parts of the program are implemented in Octave including the CMA-ES function. The interface between Octave and the process simulation provided by the Windows Component Object Model is wrapped as a function in Octave, which takes the process variables as input and returns the objective function. This function is provided as input to the CMA-ES algorithm. Inside the simulation wrapper the constraints of the separator pressures are checked. In case of violation, the wrapper function does not call the simulation and instead returns NaN as described previously. If the separator pressure constraints are not violated, the process simulation is called and calculated parameters are returned. Based on the returned parameters, the objective/profit function is calculated. If the RVP constraint is violated, the objective function is penalized before being returned to the CMA-ES function. This procedure is repeated iteratively until the stopping criteria are met. For each of the reservoir fluids investigated, 20 repetitive runs as described above are performed with the CMA-ES optimization algorithm.

Results and discussion

Gas condensate

The results for the optimization performed for the gas condensate fluid are reported in Table 4. Besides the bounded variables and the objective function also the main constraint function, RVP, as well as the total power requirement are tabulated. For illustration, the behavior in model factors and objective as a function of the number of function evaluations are depicted for a single optimization run in Figure 4.

Some unambiguous results are obtained as well as some more ambiguous results. Starting with the similarities between the optimization runs, it is observed that the objective function is maximized when the first stage separator (S1) pressure (P_S1) is at its maximum, the third stage separator (S3) pressure (P_S3) is at approx. 180 kPa, the first stage separator

Table 4: Optimization results for the gas condensate case for 20 runs with the CMA-ES optimization algorithm. μ is the average, σ is the standard deviation and σ (%) is the standard deviation relative to the average.

Run (#)	P_S1 (kPa)	P_S2 (kPa)	P_S3 (kPa)	T_S11 (°C)	T_S21 (°C)	T_S31 (°C)	T_S1 (°C)	T_S2 (°C)	T_S3 (°C)	RVP (psia)	Power (kJ/kg)	Obj ($/kg feed)
1	3497	1516	180	31.9	25.0	34.1	33.0	50.4	60.0	11.99	149.5	0.25237
2	3499	1503	179	25.0	25.0	37.5	33.0	55.4	60.0	11.98	148.8	0.25261
3	3500	1573	180	36.4	25.0	26.9	33.0	57.7	60.0	11.97	147.4	0.25237
4	3499	1410	179	40.6	25.0	67.8	33.0	37.8	60.0	11.96	158.7	0.25217
5	3500	1407	179	38.8	25.0	66.9	33.0	46.6	60.0	11.99	155.1	0.25223
6	3500	1484	180	36.8	25.0	36.6	33.0	54.9	60.0	11.99	149.6	0.25233
7	3499	1568	180	44.1	25.0	29.7	33.0	55.6	60.0	11.99	152.3	0.25236
8	3500	1603	180	31.6	25.0	25.4	33.0	55.9	60.0	11.99	146.9	0.25246
9	3494	1464	180	65.3	25.1	40.0	33.0	54.9	60.0	11.99	158.3	0.25217
10	3500	1440	179	47.0	25.0	43.9	33.0	60.0	60.0	12.00	152.9	0.25230
11	3498	1512	180	25.0	25.1	33.4	33.0	48.3	60.0	11.99	146.3	0.25255
12	3500	1611	180	40.0	25.0	27.1	33.0	53.9	60.0	11.99	152.2	0.25242
13	3489	1416	179	33.8	25.0	65.4	33.0	59.8	60.0	11.98	152.2	0.25228
14	3500	1577	181	25.0	25.2	25.0	33.0	60.0	60.0	11.99	141.8	0.25260
15	3498	1505	180	25.0	25.2	32.2	33.0	43.8	60.0	11.96	145.3	0.25246
16	3500	1410	179	62.5	25.0	52.7	33.0	55.8	60.0	12.00	159.2	0.25224
17	3493	1414	180	35.2	25.0	50.2	33.0	38.9	60.0	11.99	153.5	0.25219
18	3500	1447	179	51.5	25.2	46.7	33.0	50.9	59.9	11.99	157.7	0.25227
19	3498	1597	180	32.7	25.1	25.7	33.0	50.0	60.0	11.99	147.8	0.25242
20	3496	1453	179	55.6	25.1	46.9	33.0	54.2	60.0	11.98	159.1	0.25221
μ	3498	1495	180	39.2	25.0	40.7	33.0	52.2	60.0	11.98	151.7	0.25235
σ	2.8	71.7	0.7	12.0	0.1	14.0	0.0	6.4	0.0	0.0109	5.1	0.0001
σ (%)	0.08	4.80	0.40	30.69	0.29	34.48	0.02	12.34	0.04	0.09	3.38	0.05

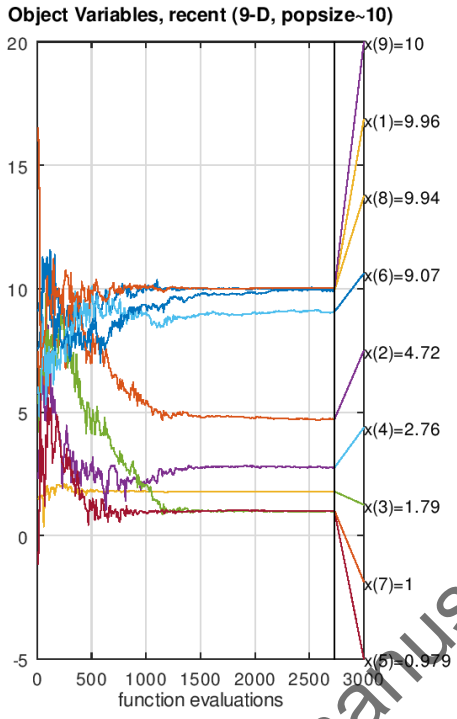

Figure 4: Results from CMA-ES for the gas condensate case (Run 15). Variables from Table 3 are shown scaled.

(S1) temperature (T_S1) is at its minimum and the third stage separator (S3) temperature (T_S3) is at its maximum. The second stage suction scrubber temperature (T_S21) is at the minimum boundary. This is also reflected in the reported standard deviation for the mentioned variables. The other variables, which include the second stage separator (S2) pressure (P_S2), the first and third stage scrubber temperatures (T_S11, T_S31), as well as the second stage separator (S2) temperature (T_S2), all display a significant variance in results between optimization runs. Apparently, this suggests, that for some variables unique settings are required to obtain an optimum, whereas other variables are allowed more variance without deteriorating the optimum value. This observation is similar to that recently reported by Andreasen.[5] Of the 20 runs, run no. 2 is the candidate with the highest objective function. This run has the optimum objective function with a second stage separator pressure (P_S2) of 1503 kPa, a first stage suction scrubber temperature (T_S11) of 25°C (lower bound), a third stage suction scrubber temperature of 37.5°C and a second

stage separator temperature of (T_S2) of 55.4°C.

It is also observed that the optimum objective function is obtained at an RVP of 12 psia (upper constraint). The RVP = 12 psia coinciding with the optimum objective can be explained by the condensate export volume being maximized when a high(er) volatility is allowed, thereby allowing more of the C_2–C_4 to be dissolved in the liquid export. Turning to the variables with unique settings again, the high pressure setting in the first stage separator can be rationalized in terms of a minimization of the compression cost (energy and hence fuel gas being subtracted from the sales gas revenue) for the compressors downstream the first stage separator (S1), i.e. the booster compressor after the scrubber S11 and the gas export compressor downstream the scrubber S12. The temperature in the separation train is going from the lowest value (S1) to the highest value (S3) with the temperature in the second stage separator being somewhere in between. This is to some extent in analogy with a distillation column with a reboiler and a reflux condenser, where the bottom stage is hottest and the top stage is coldest, giving the best separation. The pressure in the third stage separator (S3) is in the lower range, but not at the limit. The main function is to ensure that the RVP constraint is not violated, since apparently the temperature is a stronger measure in ensuring a higher condensate volume without violating the RVP constraint for applied bounds.

With respect to the temperature in the first separation stage, it might require a substantial cooling demand to obtain a temperature as low as 33°C, especially if the flowing wellhead temperature is high. This will have knock-on effects on inlet cooler size and the required flow of cooling medium. Another challenge for a low separator temperature may also be poor separation due to e.g. higher viscosity. This may result in poor oil/water separation (not included in the present study), or gas being carried over to the liquid phase. While the probabilistic optimization has provided 20 different optimizations with at least some of the variables having different settings, it is observed that the achieved optimum for the objective function is fairly invariant. The difference between the found optima is seen on the 4^{th} significant digit.

Black oil

The results for the optimization performed for the black oil fluid are reported in Table 5. For illustration, the behavior in model factors and objective as a function of the number of function evaluations are depicted for a single optimization run in Figure 5.

Table 5: Optimization results for the black oil case for 20 runs with the CMA-ES optimization algorithm.μ is the average, σ is the standard deviation and σ (%) is the standard deviation relative to the average.

Run (#)	P_S1 (kPa)	P_S2 (kPa)	P_S3 (kPa)	T_S11 (°C)	T_S21 (°C)	T_S31 (°C)	T_S1 (°C)	T_S2 (°C)	T_S3 (°C)	RVP (psia)	Power (kJ/kg)	Obj ($/kg feed)
1	2671	534	313	42.4	26.9	41.4	33.0	33.1	60.0	11.99	32.8	0.43430
2	3266	3000	357	56.9	25.0	40.3	33.0	39.2	60.0	12.00	33.7	0.43456
3	3388	600	312	25.0	53.2	60.7	33.0	33.0	60.0	12.00	29.4	0.43437
4	3081	709	317	48.6	30.5	68.6	33.0	40.9	60.0	12.00	30.8	0.43418
5	2999	582	312	32.5	49.0	25.1	33.0	33.1	60.0	12.00	31.0	0.43437
6	3112	3000	350	30.6	25.0	48.1	33.0	59.4	60.0	12.00	32.5	0.43466
7	3417	1004	323	68.1	25.0	31.5	33.0	48.0	60.0	12.00	29.6	0.43416
8	2997	621	314	29.3	30.1	48.6	33.0	35.0	60.0	12.00	30.4	0.43429
9	3130	1276	330	64.9	25.0	29.5	33.0	38.1	60.0	11.99	30.3	0.43414
10	3253	621	312	50.8	53.5	25.0	33.0	33.0	60.0	11.99	30.9	0.43436
11	3287	594	312	36.7	69.4	45.5	33.0	33.0	60.0	12.00	30.6	0.43432
12	2931	544	313	34.7	49.2	25.1	33.0	33.0	60.0	12.00	31.5	0.43437
13	2615	748	321	54.4	62.5	52.5	33.1	45.1	60.0	11.99	33.6	0.43408
14	3071	3000	352	58.6	25.0	41.8	33.0	54.5	60.0	11.99	34.2	0.43461
15	3173	559	312	46.9	66.5	64.8	33.0	33.0	60.0	11.99	31.6	0.43432
16	2906	554	313	33.8	27.3	64.2	33.0	33.0	60.0	12.00	31.2	0.43433
17	3349	573	313	50.4	54.2	25.0	33.0	33.0	60.0	12.00	30.9	0.43436
18	3105	576	312	31.8	27.6	36.5	33.0	33.0	60.0	12.00	30.2	0.43434
19	3203	3000	350	55.3	25.0	42.7	33.0	56.5	60.0	11.98	33.3	0.43462
20	3184	576	312	66.9	47.9	68.5	33.0	33.1	60.0	12.00	32.2	0.43431
μ	3107	1134	323	45.9	39.9	44.3	33.0	40.0	60.0	12.00	31.5	0.43435
σ	207.7	973.7	16.0	13.5	16.0	15.1	0.0	9.8	0.0	0.0053	1.4	0.0002
σ (%)	6.68	85.90	4.95	29.50	40.20	34.06	0.10	24.60	0.00	0.04	4.48	0.04

To begin with, there are both similarities with the gas condensate results as well as distinct differences. The main similarity is the RVP = 12 psia and unique settings in terms of temperature on the first (S1) and third stage (S3) separators with the temperature in the former being at its lowest value and the latter being at its highest value again. The first and third stage condenser/suction scrubber temperatures are again non-unique. The same applies to the temperature in the second stage separator (S2). The difference between the found optima for the different optimization runs is seen on the 4^{th} significant digit.

The main difference is that the parameters which had unique settings for the gas conden-

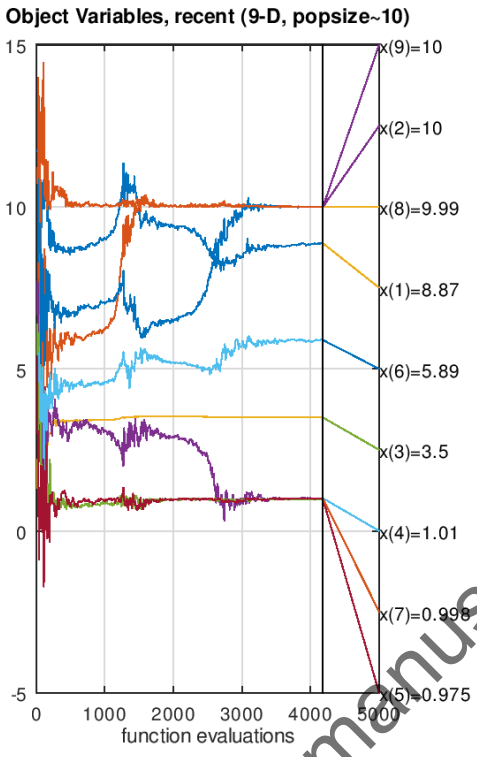

Figure 5: Results from CMA-ES for the black oil case (Run 18). Variables from Table 3 are shown scaled.

sate case, i.e. the first stage separator (S1) pressure (P_S1) and the third stage separator (S3) pressure (P_S3), do not appear to display as unique settings, as seen from the variance reported in Table 5. The standard deviation is now 5-7 % percent. The first stage separator pressure is also lower in average by approx. 400 kPa, whereas the third stage separator pressure is higher in average by 143 kPa. The second stage separator pressure varies greatly from either close to the lower bound or at the upper bound, with no values in between. The second stage condenser/scrubber that had unique settings for the gas condensate case now has a significant variance between runs. A further distinct difference is also the higher value of the optimal objective function. This is a direct consequence of the higher fraction of liquid per unit feed, and the liquid export being the higher value stream.

It is interesting to observe that the first stage separator pressure is not at its upper bound, since this minimizes power consumption and thereby loss of gas export revenue (due

to subtraction of fuel gas). One speculative explanation can be that the gas export (and power required for compression) has a lower weight in the total revenue. Thus, even a slightly higher energy consumption for gas compression can be tolerated if it actually can increase the liquid volume export.

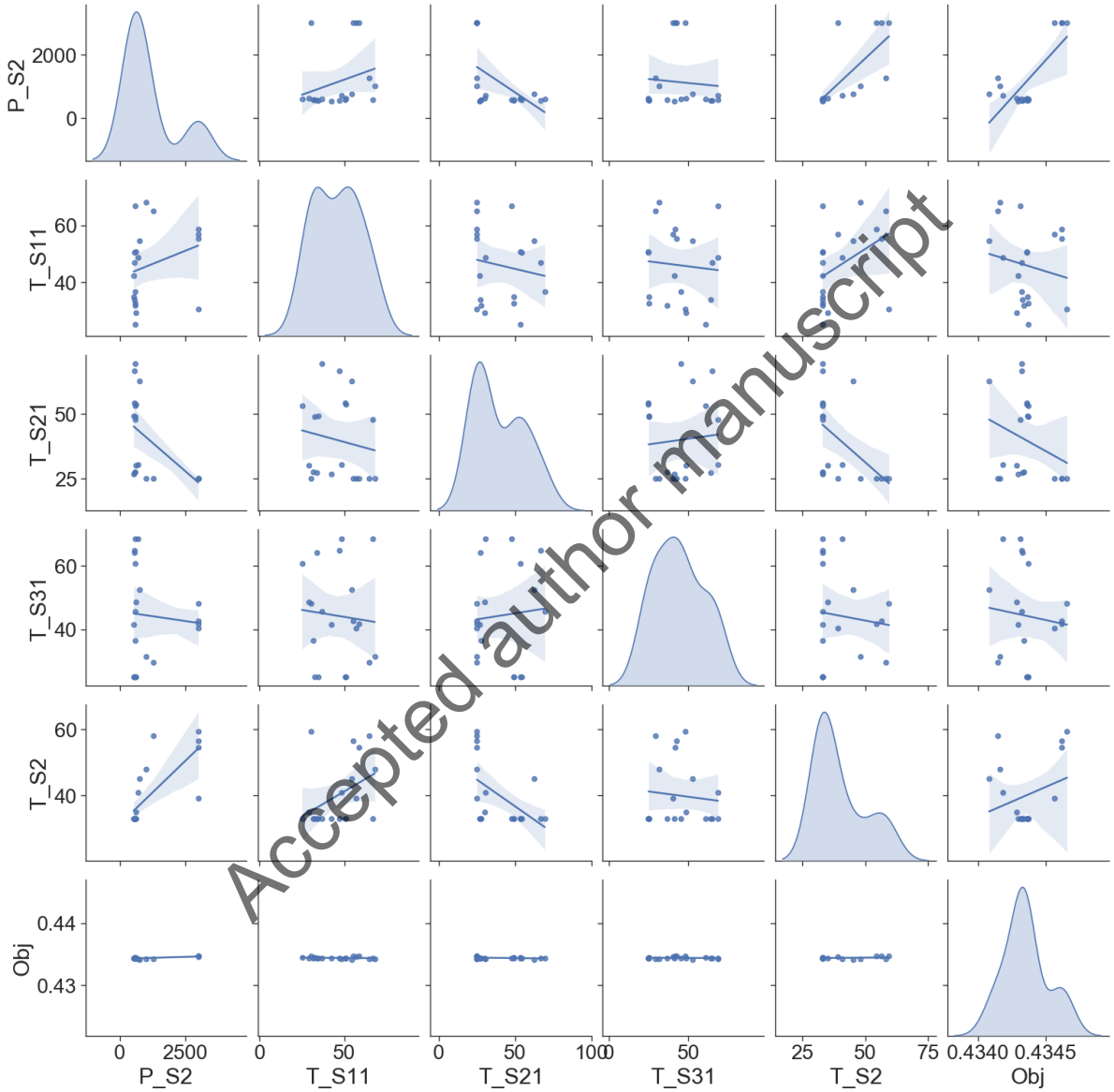

Figure 6: Pair plot for variables with large variation for the black oil optimization.

The results for the variables with large variances are analyzed in more detail in the pair plot in Figure 6. As seen from the Kernel Density estimate of the probability density function for the objective function, it appears that the obtained maximum objective has

some clustering. This is also observed for the second stage separator pressure P_S2, as also briefly mentioned above, with the best candidates among the 20 runs being the ones with the pressure at the higher bound. Furthermore, it is also noted that the maximum objective function is obtained when the temperature in the second stage condenser/scrubber is at the lower bound. The best candidate along the 20 runs is no. 6.

In order to get a clearer picture of the best settings, the runs with low second stage separator pressure are filtered out from Table 5 and the statistics are recalculated for the reduced number of runs. The results are summarized in Table 6. It is worth highlighting that after filtering out the runs with low second stage separator pressure, the only variables which remain with a substantial variance (T_S11, T_S31, T_S2) are the same as those showing a high variance for the gas condensate.

Table 6: Filtered optimization results for the black oil case. μ is the average, σ is the standard deviation and σ (%) is the standard deviation relative to the average.

Run (#)	P_S1 (kPa)	P_S2 (kPa)	P_S3 (kPa)	T_S11 (°C)	T_S21 (°C)	T_S31 (°C)	T_S1 (°C)	T_S2 (°C)	T_S3 (°C)	RVP (psia)	Power (kJ/kg)	Obj ($/kg feed)
2	3266	3000	357	56.9	25.0	40.3	33.0	39.2	60.0	12.00	33.7	0.43456
6	3112	3000	350	30.6	25.0	48.1	33.0	59.4	60.0	12.00	32.5	0.43466
14	3071	3000	352	58.6	25.0	41.8	33.0	54.5	60.0	11.99	34.2	0.43461
19	3203	3000	350	55.3	25.0	42.7	33.0	56.5	60.0	11.98	33.3	0.43462
μ	3163	3000	352	50.3	25.0	43.2	33.0	52.4	60.0	11.99	33.4	0.43461
σ	76.3	0.0	3.4	13.3	0.0	3.4	0.0	9.1	0.0	0.0106	0.7	0.0000
σ (%)	2.41	0.00	0.96	26.33	0.00	7.85	0.07	17.28	0.00	0.09	2.20	0.01

Volatile oil

The results for the optimization performed for the volatile oil fluid are reported in Table 7. For illustration, the behavior in model factors and objective as a function of the number of function evaluations are depicted for a single optimization run in Figure 7.

As seen from Table 7, the case with volatile oil has a few things in common with both the gas condensate and the black oil cases. The first and third stage separator temperatures, T_S1 and T_S3, are at the low and high bound, respectively. Furthermore, the third stage separator pressure P_S3 has a low variance. The first stage separator pressure P_S1 is near

Table 7: Optimization results for the volatile oil case for 20 runs with the CMA-ES optimization algorithm. μ is the average, σ is the standard deviation and σ (%) is the standard deviation relative to the average.

Run (#)	P_S1 (kPa)	P_S2 (kPa)	P_S3 (kPa)	T_S11 (°C)	T_S21 (°C)	T_S31 (°C)	T_S1 (°C)	T_S2 (°C)	T_S3 (°C)	RVP (psia)	Power (kJ/kg)	Obj ($/kg feed)
1	3488	1852	194	40.8	25.1	54.8	33.0	55.8	59.9	11.98	93.1	0.39647
2	3467	1833	195	57.3	25.0	63.9	33.0	59.5	60.0	11.98	92.1	0.39643
3	2168	1710	194	33.1	25.1	34.7	33.0	54.4	60.0	11.97	99.0	0.39579
4	3469	1925	195	25.2	25.0	28.2	33.0	51.4	60.0	11.98	89.1	0.39661
5	2648	336	200	59.2	68.6	65.7	33.0	33.0	60.0	12.00	76.4	0.39362
6	3265	1798	194	34.9	25.0	58.2	33.1	56.4	60.0	12.00	91.8	0.39649
7	2905	1750	195	32.6	25.0	38.9	33.0	41.1	60.0	11.99	93.0	0.39627
8	2659	344	200	57.6	66.2	56.7	33.0	33.0	60.0	12.00	75.8	0.39363
9	2661	333	200	41.5	49.5	52.9	33.0	33.0	60.0	12.00	73.2	0.39365
10	2689	1745	193	54.1	25.1	46.6	33.0	46.4	60.0	12.00	103.7	0.39627
11	3480	1865	196	50.4	25.0	34.1	33.0	43.9	60.0	11.99	90.1	0.39642
12	3370	1873	194	25.0	25.2	41.5	33.0	50.0	60.0	11.98	95.3	0.39649
13	2633	335	200	47.7	54.8	57.6	33.0	33.0	60.0	12.00	74.5	0.39364
14	2863	1747	194	39.3	25.0	38.3	33.0	57.9	60.0	11.99	90.1	0.39633
15	2616	336	200	41.1	61.3	51.0	33.0	33.0	60.0	12.00	74.0	0.39364
16	2613	336	200	57.8	69.3	68.9	33.0	33.0	60.0	12.00	76.5	0.39362
17	3278	1877	194	34.0	25.1	29.9	33.0	59.7	60.0	11.97	87.3	0.39647
18	3242	1824	195	37.0	25.0	38.6	33.0	49.0	60.0	12.00	92.7	0.39647
19	3399	1815	196	55.1	25.1	47.0	33.0	45.6	60.0	12.00	92.2	0.39640
20	3297	1865	196	57.3	25.0	27.3	33.0	57.7	60.0	11.99	86.5	0.39646
μ	3010	1375	196	44.1	36.0	46.7	33.0	46.4	60.0	11.99	87.3	0.39556
σ	393.6	699.4	2.5	11.4	17.7	12.9	0.0	10.3	0.0	0.0109	9.1	0.0013
σ (%)	13.07	50.87	1.25	25.96	49.04	27.57	0.04	22.25	0.02	0.09	10.38	0.33

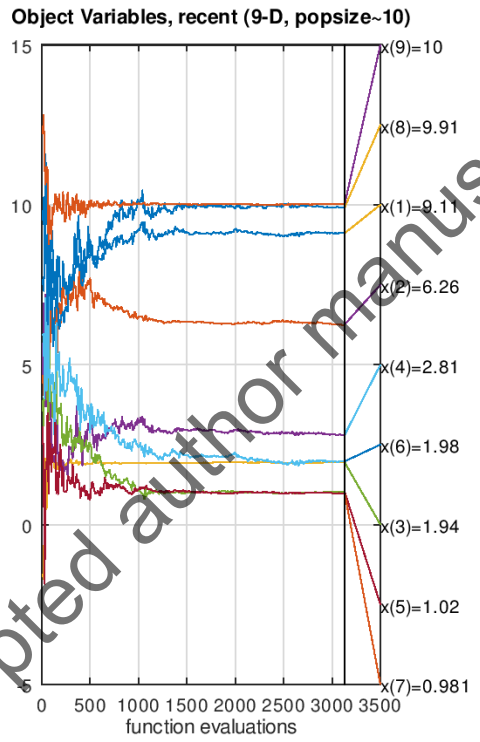

Figure 7: Results from CMA-ES for the volatile oil case (Run 18). Variables from Table 3 are shown scaled.

the high boundary but has some variance.

All other parameters have a significant variance including the objective function and the specific power consumption. In order to investigate this in more detail, a pair plot is used for the volatile oil results for the parameters with the largest variance. This is shown in Figure 8.

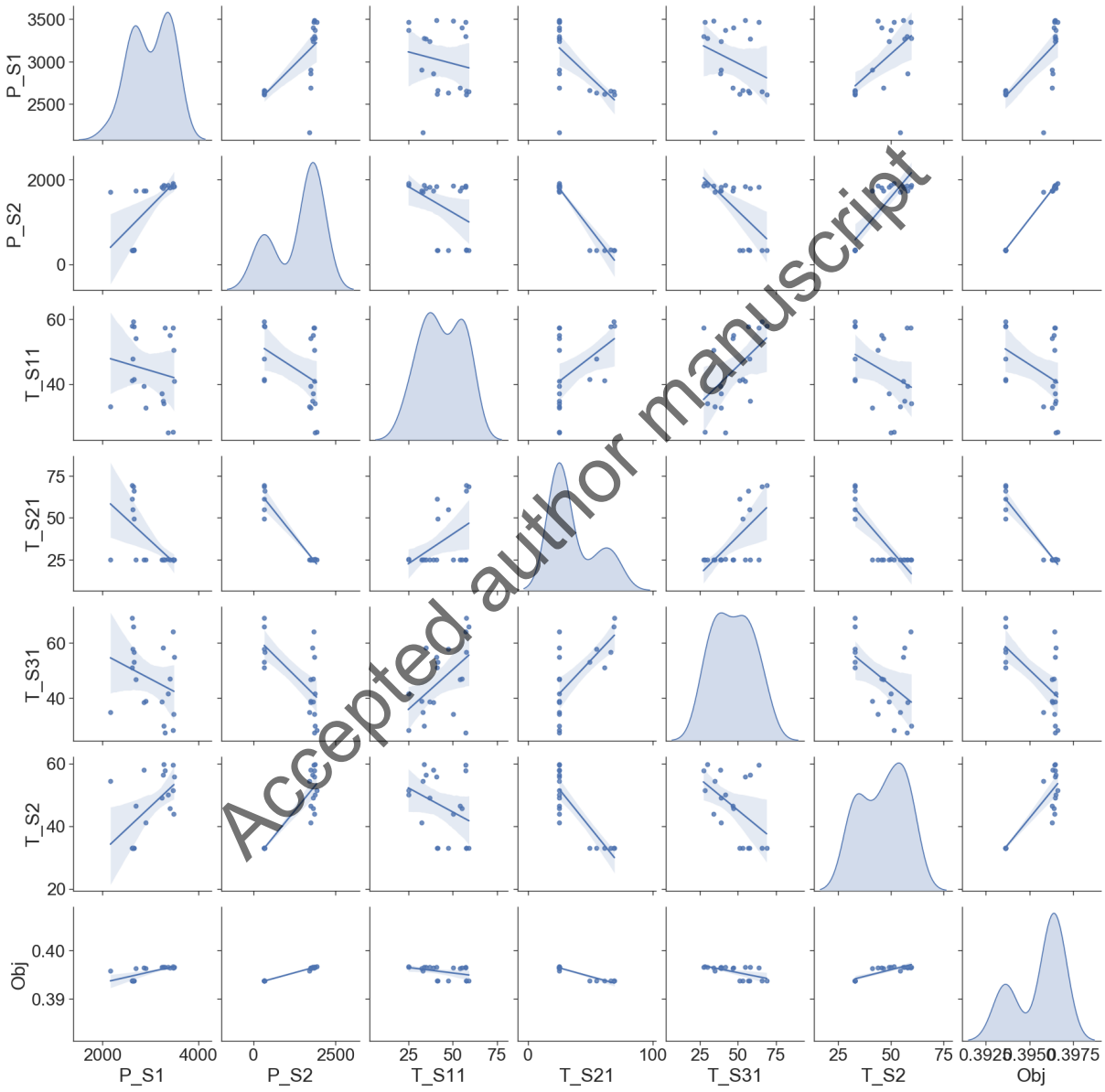

Figure 8: Pair plot for parameters with largest variance for the volatile oil case.

From Figure 8, a clear clustering is observed for e.g. the second stage separator pressure, P_S2, the temperature in the second stage condenser/scrubber, T_S21, and the objective

function. It is observed that the maximum value of the objective function is favored by the second stage separator pressure being at a value from 1750 – 1925 kPa and with a second stage condenser/scrubber temperature being at the lower bound. Filtered results, leaving out the sub-optimal runs, are compiled in Table 8. The filtered results give more unambiguous results in terms of selecting optimal settings for providing maximum profit, though some variables still have some freedom to be set at different values without significantly deteriorating the obtainable profit. Also in this case, after filtering out, the variables remaining with a substantial variance are T_S11, T_S31 and T_S2, as in the other two cases. In this case, however, P_S1 also keeps a relatively high variance. Apparently, some variables have a higher variance by nature, or allowed by the process, whereas the high variance in the unfiltered results for some parameters is due to the optimization not finding a global maximum in some cases e.g. due to its stochastic nature combined with insufficient population size, coarse stopping criteria etc. The candidate with the highest value of the objective function is run no. 4.

Table 8: Filtered optimization results for the volatile oil case. μ is the average, σ is the standard deviation and σ (%) is the standard deviation relative to the average.

Run (#)	P_S1 (kPa)	P_S2 (kPa)	P_S3 (kPa)	T_S11 (°C)	T_S21 (°C)	T_S31 (°C)	T_S1 (°C)	T_S2 (°C)	T_S3 (°C)	RVP (psia)	Power (kJ/kg)	Obj ($/kg feed)
1	3488	1852	194	40.8	25.1	54.8	33.0	55.8	59.9	11.98	93.1	0.39647
2	3467	1833	195	57.3	25.0	63.9	33.0	59.5	60.0	11.98	92.1	0.39643
3	2168	1710	194	33.1	25.1	34.7	33.0	54.4	60.0	11.97	99.0	0.39579
4	3469	1925	195	25.2	25.0	28.2	33.0	51.4	60.0	11.98	89.1	0.39661
6	3265	1798	194	34.9	25.0	58.2	33.1	56.4	60.0	12.00	91.8	0.39649
7	2905	1750	195	32.6	25.0	38.9	33.0	41.1	60.0	11.99	93.0	0.39627
10	2689	1745	193	54.1	25.1	46.6	33.0	46.4	60.0	12.00	103.7	0.39627
11	3480	1865	196	50.4	25.0	34.1	33.0	43.9	60.0	11.99	90.1	0.39642
12	3370	1873	194	25.0	25.2	41.5	33.0	50.0	60.0	11.98	95.3	0.39649
14	2863	1747	194	39.3	25.0	38.3	33.0	57.9	60.0	11.99	90.1	0.39633
17	3278	1877	194	34.0	25.1	29.9	33.0	59.7	60.0	11.97	87.3	0.39647
18	3242	1824	195	37.0	25.0	38.6	33.0	49.0	60.0	12.00	92.7	0.39647
19	3399	1815	196	55.1	25.1	47.0	33.0	45.6	60.0	12.00	92.2	0.39640
20	3297	1865	196	57.3	25.0	27.3	33.0	57.7	60.0	11.99	86.5	0.39646
μ	3170	1820	195	41.2	25.1	41.6	33.0	52.1	60.0	12.0	92.6	0.39638
σ	383.2	62.7	0.8	11.6	0.1	11.3	0.0	6.2	0.0	0.0	4.5	0.00019
σ (%)	12.09	3.44	0.42	28.09	0.26	27.15	0.05	11.83	0.03	0.09	4.86	0.05

Comparison between fluids

The results of the optimal plant settings for the three fluids investigated are summarized in Figure 9. The graphs show the best candidates from the repetitive optimizations runs.

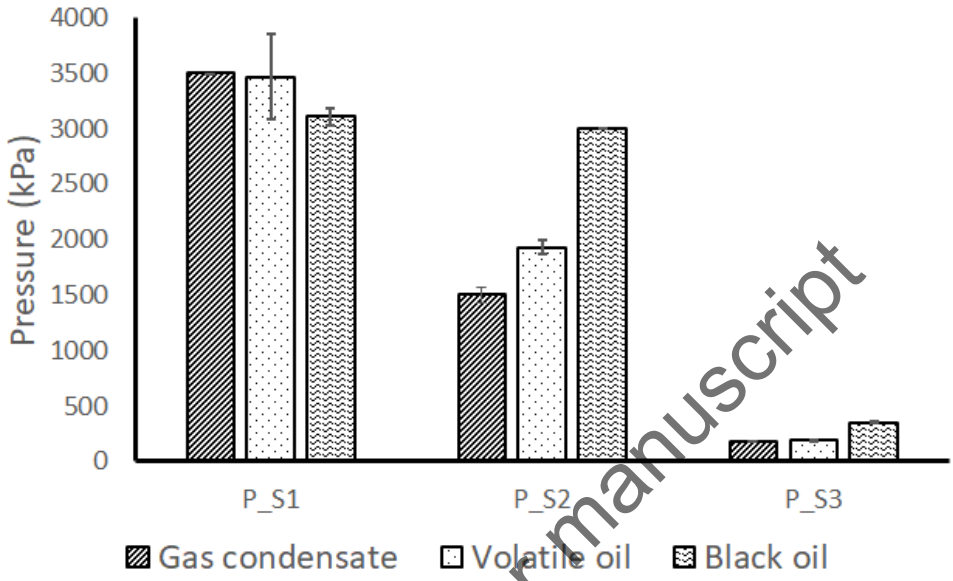

(A)

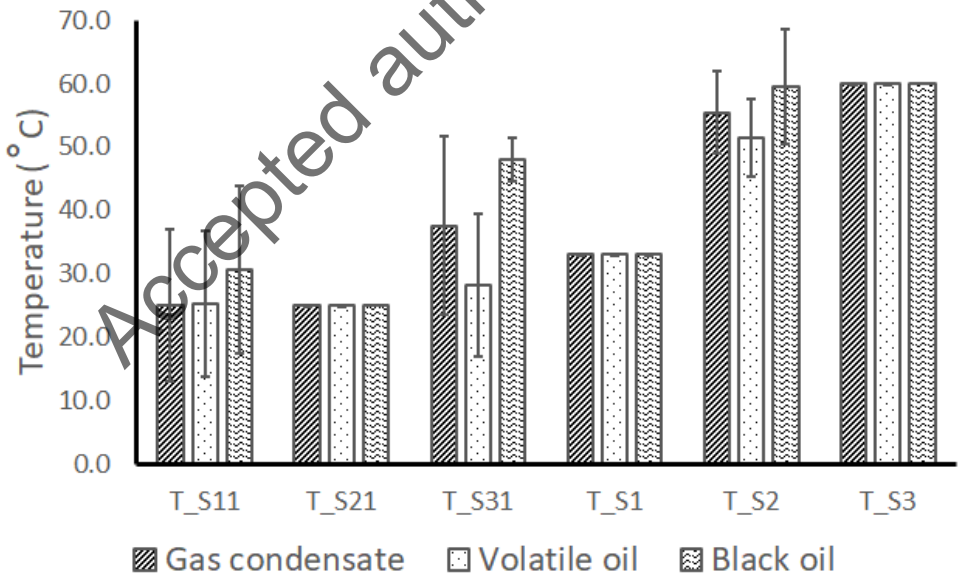

(B)

Figure 9: Comparison of optimal parameter settings for the three fluids investigated, showing (A) optimal separator pressures and (B) optimal temperature settings. Error bar magnitude is equal to one standard deviation as found from the repetitive optimization runs. For the black oil and the volatile oil the standard deviation is derived for the filtered runs.

For the first stage separator pressure, P_S1, there is an apparent tendency for a declining optimal pressure going from gas condensate, over volatile oil to the black oil case. However, the volatile oil has a significant variance. For the second stage separator pressure, P_S2, as well as the third stage separator pressure, P_S3, there is a trend of increasing pressure for the optimal settings, cycling over gas condensate, volatile oil and black oil, in that order. The black oil is apparently a special case with the second stage separator having the optimal pressure at the upper bound, with little difference from the first stage separator. One could argue that this effectively renders the oil and gas separation as a two-stage separation, with very little load on the second stage separator. This could be interesting to analyze in more detail in future studies. One caveat though is that the re-compression of the gas from the third stage separator in order to be commingled with gas from the second stage separator requires a very high compression ratio. Such a high compression ratio will require a two-stage compression process with inter-stage cooling and condensate knock-out.

As already described for all three fluids, the temperature in the first stage separator, T_S1, is optimal at the lower boundary while optimal at the high boundary for the third stage separator temperature, T_S3. The second stage separator pressure is optimal in the high end between 50 and 60°C for all fluids, with some variation for the optimal cases between the different fluids, but considering the variance it is difficult to conclude on a significant trend. The variance itself indicates that some freedom to set the temperature is available without significantly reducing the objective function.

With respect to the temperature in the condensers/scrubbers in the compression train, a temperature at the lower boundary is favored for all three fluids. For the first stage separator, a low temperature is favored, but like the temperature in the second stage separator, significant variance is found between repetitive optimization runs. For the third stage condenser/scrubber, T_S31, at least it seems that a higher temperature is required for the black oil compared to the volatile oil. Both the gas condensate and the volatile oil displays large variance, again indicating some freedom in setting this temperature.

Optimization potential

A large effort has been made in order to optimize the profit for the three fluids investigated, yet in lack of a reliable and realistic baseline, it is not known exactly how much this optimization is worth. Obviously, the performance of any optimization depends on the baseline when benchmarked. The models and parameters employed in the present study do not resemble any existing real separation plants from which a baseline can be defined. As an alternative, a baseline will be defined by performing separate optimization runs, but now with the constraints that the first stage separator pressure shall be at the high boundary and that the pressure in the second stage separator shall be given by $P_{S2} = \sqrt{P_{S1}P_{S3}}$ (geometric mean). The geometric mean is a common rule of thumb applied for optimal intermediate separator pressure.[15] Furthermore, the RVP shall be at least 11.9 psia, but still below or equal to 12 psia. Otherwise, all other parameters are subject to the same boundaries as defined in Table 3. As a difference to the previously defined optimization problems, now the objective is to find the lowest (worst) objective function value. This baseline will be named "best case" i.e. the baseline showing the largest potential for optimization as compared to the optimal cases found in the previous sections. Another scenario with the same constraints on P_S1 and P_S2, but now with the target to find the largest profit/best objective function, is used as another baseline. This is named "realistic case".

The relative change in profit/objective function from the two baselines defined in the previous paragraph to the best candidates as found in the previous section is shown in Figure 10 (A). Note that positive changes reflect a reduction in the objective function with respect to the best optimum found. The results show that apparently the gas condensate case has the largest potential for optimization in terms of maximizing profit considering the "best case" baseline. The optimization potential decreases for the volatile oil and the black oil in that order. Considering the "realistic case", where partial optimization has been done, and which therefore might better represent a real starting point for optimization, the optimization potential is obviously less. Now the gas condensate and volatile oil are comparable in the

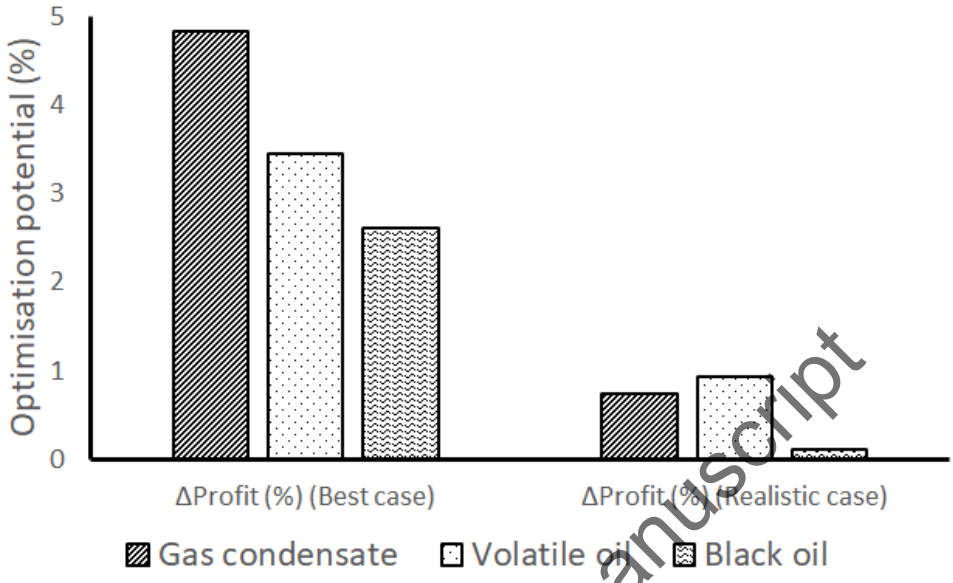

(A)

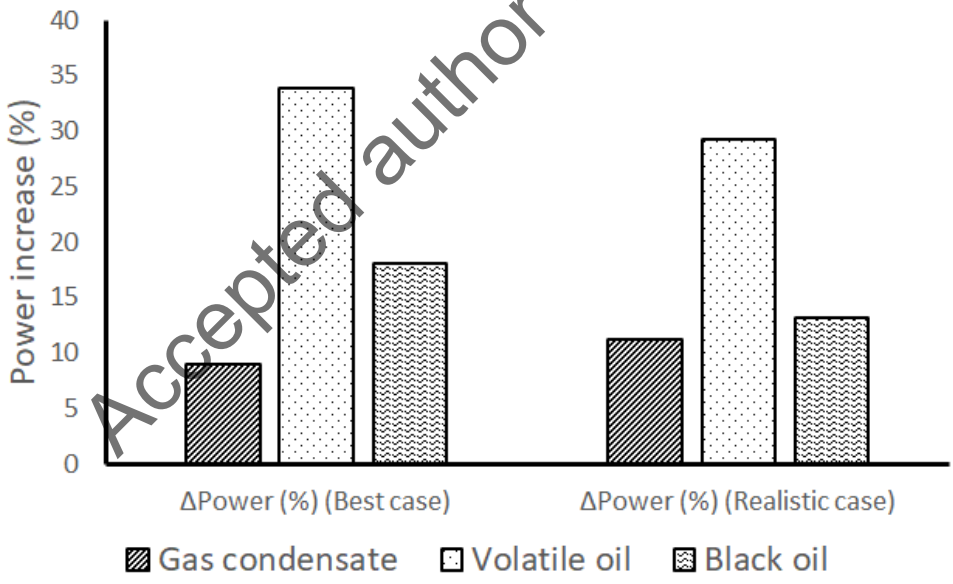

(B)

Figure 10: Realized change (decrease/improvement) in objective function/profit (A) from the defined baselines to the optimal candidates and (increase/deterioration) in power consumption.

magnitude of realized optimization potential (0.7% and 0.9%, respectively), whereas a much lower optimization potential seems realizable for the black oil case (0.1%). The magnitude of the realizable optimization potential is notoriously dependent on the baseline; however, a comparison has previously been made by Andreasen[7] including results from other studies.[3,10,13,14] The potential for optimization in either stabilized oil export or total profit seems to be in the range from 0.1–2.0 %. The defined "realistic case" baseline showing a potential of 0.1–0.9% seems to be very much in line with this range of optimization potentials.

Figure 10 (B) shows the concurrent increase in power requirement when going from the defined baseline scenarios to the same optimal solutions as used for comparing profit/objective function optimization. These results are very interesting, since a huge difference in power requirement is seen. The results clearly show that it is very costly in terms of power requirement to optimize the operating profit which to a large extent is controlled by the amount of well fluid recovered as liquid export. Even for the "realistic case" baseline for the volatile oil, an increase in power of 30% is seen for an increase in profit of 0.9%. It has been observed and noted by others that the amount of condensation taking place in the gas compression/treatment system can have a huge effect on the power requirement for compression.[7,37] The rationale is that condensate formed during cooling in the compressor suction coolers or due to hydrocarbon dew point control (not modeled in the present study) by e.g. J-T cooling (adiabatic) or gas expanders (isentropic) is normally recycled back into the separation system, where partial evaporation takes places. The effect is a build-up of a substantial recycle, especially middle components such as C_3–C_5. This effectively increases the mass flow rate through the compressors and hence the amount of required power. This is also somewhat in analogy with distillation columns, where increased purities can be obtained increasing the reflux ratio, even though this gives increased expenses (more heat required at the reboiler, more reflux to be pumped and cooled as well as a larger column).

The increased power required for realizing the optimum operating profit has a significant impact on the facility design. Increasing compressor power results in larger compressor pack-

ages, larger suction scrubbers since more flow is handled, and larger suction scrubber coolers being required due to increased cooling demand. Again, this trickles down and impacts the cooling system which needs to offer a higher duty/more flow. The increased compression system power requirement impacts electricity generation (if supplied by gas turbine driven generators), which also increases in size. Even the size of the oil and gas separators in the separation train may be impacted by the larger liquid and vapor flow that needs handling. The required cost for designing the facility to handle this might even result in a negative NPV for the entire project development. For existing facilities, the optimal operating profit may also become difficult to realize without significant modifications to existing equipment. Limitations in installed equipment e.g. compressors, heat exchangers, separators/scrubbers may prohibit reaching a global optimum due to increasing recycle streams challenging design limits.

Taking the above considerations into account when applying multi-parameter optimization of an oil and gas separation plant, it will be beneficial to not only optimize OPEX, but equally important, to optimize CAPEX, i.e. a multi-objective optimization problem. This can be reduced to a single-objective problem by aggregating CAPEX and OPEX into a function for NPV.

Conclusion

The optimization of an oil and gas separation plant for different characteristic reservoir fluid types has been performed in this work. The oil and gas separation plant, represented by a rigorous process simulation model, consists of three separation stages, and a compression system, re-compressing the flashed gas from each separator into a common gas export compressor. Each compression stage includes a suction cooler and a scrubber upstream a compressor. The suction cooler allows cooling and partial condensation of the flash gas. Any liquids condensing in the suction scrubbers are fed back into the separation train. The three

fluids show some similarities in their optimal settings:

- The temperature in the first stage separator is optimal at the low bound.
- The temperature in the third (final) stage separator is optimal at the high bound.
- The temperature in the second stage separator is optimal in the higher range towards the upper bound, but with significant variation across repeated optimization runs, indicating some flexibility in setting this temperature.
- The temperature in the scrubber/condenser before compression of the gas from the middle stage separator is optimal at the low bound.
- The temperature in the first stage condenser/scrubber is optimal near or at the low bound, but there is a significant variation between consecutive optimization runs, indicating that there is some degree of freedom in setting this parameter without significantly deteriorating the optimum.

The following general trends are found:

- The pressure in the first stage separator is optimal at the high bound for the gas condensate case. For the volatile oil and the black oil cases, the optimal separator pressure is lower and decreasing in the order of decreasing GOR. However, volatile oil optimal setting has a significant variance indicating that the optimum of the objective function is less sensitive to the exact value.
- The optimal pressure in the second stage separator generally increases in the order of decreasing GOR of the fluid optimized, i.e. the order is: gas condensate, volatile oil and black oil.
- The optimal pressure in the third stage separator generally increases in the order of decreasing GOR of the fluid optimized, i.e. the order is: gas condensate, volatile oil and black oil.

In terms of an estimated optimization potential, it is found that for at least the gas condensate and the volatile oil, depending on the quality of the starting point, the operating profit from product sales can be increased by close to 1% by performing a plant-wide optimization using an evolutionary algorithm. For the black oil, the optimization potential is much less, but still significant. It is also noticed that the maximization of operating profit comes at a cost of increased power consumption, due to increased internal recycles of middle components/NGL. This is most pronounced for the volatile oil. This information is very useful and can be exploited for a minimization of the environmental footprint through reduced fuel gas combustion for power generation. The competing forces of power requirements and production optimization should be explored in greater detail in future studies using e.g. multi-objective optimization and Pareto analysis.

Acknowledgement

The authors thank Honeywell for providing an academic license for the UniSim Design process simulation software. Language secretary Susanne Tolstrup is acknowledged for proofreading the manuscript.

Abbreviations

ANN	Artificial Neural Networks
CAPEX	Capital Expenditure
CMA-ES	Covariance Matrix Adaption Evolution Strategy
COM	(Windows) Component Object Model
COSTALD	Corresponding State Liquid Density
EA	Evolutionary Algorithm
EOS	Equation of State
FPSO	Floating Production Storage Offloading Vessel
GA	Genetic Algorithm
GOR	Gas Oil Ratio
LHV	Lower Heating Value
LNG	Liquefied Natural Gas
NGL	Natural Gas Liquids
NPV	Net Present Value
NSGA	Non-dominant Sorting Genetic Algorithm
OFAT	One Factor At a Time
OPEX	Operational Expenditures
PFD	Process Flow Diagram
PH	Pressure-Enthalpy (flash)
PVT	Pressure, Volume and Temperature
PWO	Plant-wide Optimization
RSM	Response Surface Model/Methodology
RVP	Reed Vapor Pressure
SG	Specific gravity
SLSQP	Sequential Least SQuares Programming
SQP	Sequential Quadratic Programming
TVP	True Vapor Pressure
UDF	User Defined Flash/Function
VBA	Visual Basic for Application

References

(1) Bothamley, M. Offshore processing options vary widely. *Oil & Gas Journal* **2004**, *102*, 47–55.

(2) Maschietti, M. Effect of the Number of Stages and Feed Composition on Offshore Oil and Gas Separation Train. *Chemical Engineering Transactions* **2019**, *74*, 847–852.

(3) Motie, M.; Moein, P.; Moghadasi, R.; Hadipour, A. *IPTC-19396-MS*; International Petroleum Technology Conference: Beijing, China, 2019; Chapter Separator Pressure Optimisation and Cost Evaluation of a Multistage Production Unit Using Genetic Algorithm, p 14.

(4) Mahmoud, M.; Tariq, Z.; Kamal, M. S.; Al-Naser, M. Intelligent prediction of optimum separation parameters in the multistage crude oil production facilities. *Journal of Petroleum Exploration and Production Technology* **2019**, 1–17.

(5) Andreasen, A. Applied Process Simulation-Driven Oil and Gas Separation Plant Optimization Using Surrogate Modeling and Evolutionary Algorithms. *ChemEngineering* **2020**, *4*, 1–21 (Article no. 11).

(6) Allahyarzadeh-Bidgoli, A.; Dezan, D. J.; Salviano, L. O.; de Oliveira Junior, S.; Yanagihara, J. I. FPSO fuel consumption and hydrocarbon liquids recovery optimization over the lifetime of a deep-water oil field. *Energy* **2019**, *181*, 927–942.

(7) Andreasen, A.; Rasmussen, K. R.; Mandø, M. Plant Wide Oil and Gas Separation Plant Optimisation using Response Surface Methodology. *IFAC-PapersOnLine* **2018**, *51*, 178 – 184, 3rd IFAC Workshop on Automatic Control in Offshore Oil and Gas Production OOGP 2018.

(8) Allahyarzadeh-Bidgoli, A.; Salviano, L. O.; Dezan, D. J.; de Oliveira Junior, S.; Yanag-

ihara, J. I. Energy optimization of an FPSO operating in the Brazilian Pre-salt region. *Energy* **2018**, *164*, 390 – 399.

(9) Kim, I. H.; Dan, S.; Kim, H.; Rim, H. R.; Lee, J. M.; Yoon, E. S. Simulation-Based Optimization of Multistage Separation Process in Offshore Oil and Gas Production Facilities. *Industrial & Engineering Chemistry Research* **2014**, *53*, 8810—8820.

(10) Ghaedi, M.; Ebrahimi, A. N.; Pishvaie, M. R. Application of genetic algorithm for optimization of separator pressures in multistage production units. *Chemical Engineering Communications* **2014**, *201*, 926–938.

(11) Ling, K.; Wu, X.; Guo, B.; He, J. New Method To Estimate Surface-Separator Optimum Operating Pressures. *Oil and Gas Facilities* **2013**, *2*, 65–76.

(12) Al-Jawad, M. S.; Hassan, O. F. Correlating Optimum Stage Pressure for Sequential Separator Systems. *SPE Projects, Facilities & Construction* **2010**, *5*, 13–16.

(13) Kylling, Ø. W. *Optimizing separator pressure in multistage crude oil production plant (Master thesis)*; Norwegian University of Science and Technology, 2009.

(14) Bahadori, A.; Vuthaluru, H. B.; Mokhatab, S. Optimizing separator pressures in the multistage crude oil production unit. *Asia-Pacific Journal of Chemical Engineering* **2008**, *3*, 380–386.

(15) Al-Farhan, F. A.; Ayala H., L. F. Optimization of surface condensate production from natural gases using artificial intelligence. *Journal of Petroleum Science and Engineering* **2006**, *53*, 135 – 147.

(16) Bahadori, A., Ed. *Fluid Phase Behavior for Conventional and Unconventional Oil and Gas Reservoirs*; Gulf Professional Publishing: Boston, 2017.

(17) Danesh, A., Ed. *PVT and Phase Behaviour of Petroleum Reservoir Fluids*; Developments in Petroleum Science; Elsevier, 1998; Vol. 47; p 213.

(18) Peng, D.-Y.; Robinson, D. B. A New Two-Constant Equation of State. *Industrial & Engineering Chemistry Fundamentals* **1976**, *15*, 59–64.

(19) Hankinson, R. W.; Thomson, G. H. A new correlation for saturated densities of liquids and their mixtures. *AIChE Journal* **1979**, *25*, 653–663.

(20) Twu, C. H. An internally consistent correlation for predicting the critical properties and molecular weights of petroleum and coal-tar liquids. *Fluid Phase Equillibria* **1984**, *16*, 137–150.

(21) Twu, C. H.; Coon, J. E.; Cunningham, J. R. A generalized vapor pressure equation for heavy hydrocarbons. *Fluid Phase Equilibria* **1994**, *96*, 19 – 31.

(22) US Energy Information and Administration. `https://www.eia.gov/todayenergy/prices.php`, Accessed: 26 April 2020.

(23) Aspelund, A.; Gundersen, T.; Myklebust, J.; Nowak, M.; Tomasgard, A. An optimization-simulation model for a simple LNG process. *Computers & Chemical Engineering* **2010**, *34*, 1606 – 1617.

(24) Caballero, J. A.; Grossmann, I. E. An algorithm for the use of surrogate models in modular flowsheet optimization. *AIChE Journal* **2008**, *54*, 2633–2650.

(25) Hansen, N.; Auger, A.; Ros, R.; Finck, S.; Pošík, P. Comparing Results of 31 Algorithms from the Black-Box Optimization Benchmarking BBOB-2009. Proceedings of the 12th Annual Conference Companion on Genetic and Evolutionary Computation. New York, NY, USA, 2010; p 1689–1696.

(26) Szynkiewicz, P. A Comparative Study of PSO and CMA-ES Algorithms on Black-box Optimization Benchmarks. *Journal of Telecommunication and Information Technology* **2018**, *4*, 5–17.

(27) Hansen, N. The CMA Evolution Strategy: A Tutorial. 2016; https://arxiv.org/abs/1604.00772.

(28) Hansen, N.; Ostermeier, A. Completely derandomized self-adaptation in evolution strategies. *Evolutionary computation* **2001**, *9*, 159—195.

(29) Hansen, N.; Kern, S. Evaluating the CMA Evolution Strategy on Multimodal Test Functions. Parallel Problem Solving from Nature - PPSN VIII. Berlin, Heidelberg, 2004; pp 282–291.

(30) Hansen, N. In *Towards a new evolutionary computation. Advances on estimation of distribution algorithms*; Lozano, J., Larranaga, P., Inza, I., Bengoetxea, E., Eds.; Springer, 2006; pp 75–102.

(31) Ros, R.; Hansen, N. A Simple Modification in CMA-ES Achieving Linear Time and Space Complexity. Parallel Problem Solving from Nature – PPSN X. Berlin, Heidelberg, 2008; pp 296–305.

(32) Hansen, N. CMA-ES: Evolution Strategy with Covariance Matrix Adaptation for nonlinear function minimization ver. 3.61. http://cma.gforge.inria.fr/cmaes_sourcecode_page.html, 2011.

(33) MATLAB, *version 7.10.0 (R2010a)*; The MathWorks Inc.: Natick, Massachusetts, 2010.

(34) Eaton, J. W. GNU Octave and reproducible research. *Journal of Process Control* **2012**, *22*, 1433 – 1438.

(35) Eaton, J. W.; Bateman, D.; Hauberg, S.; Wehbring, R. GNU Octave version 4.4.0 manual: a high-level interactive language for numerical computations. 2018.

(36) Honeywell, *Unisim Design customization. R470 Release*; Honeywell International Sàrl, 2019.

(37) Campbell, J. M. In *Gas conditioning and processing*, 8th ed.; Hubbard, R. A., Ed.; John M. Campbell and Company, 2004; Vol. 1 – The Basic Principles.

Graphical TOC Entry